Chin. J. Astron. Astrophys. Vol. 5 (2005), No. 4, 379–398
(*http://www.chjaa.org*)

Chinese Journal of
Astronomy and
Astrophysics

# Precession of the Orbital Plane of Binary Pulsars and Significant Variabilities

Bi-Ping Gong

Department of Astronomy, Nanjing University, Nanjing 210093; *bpgong@nju.edu.cn*

Received 2004 October 10; accepted 2005 February 28

**Abstract** There are two ways of expressing the precession of orbital plane of a binary pulsar system, given by Barker & O'Connell, Apostolatos et al. and Kidder, respectively. We point out that these two ways actually come from the same Lagrangian under different degrees of freedom. Damour & Schäfer and Wex & Kopeikin applied Barker & O'Connell's orbital precession velocity in pulsar timing measurement. This paper applies Apostolatos et al.'s and Kidder's orbital precession velocity. We show that Damour & Schäfer's treatment corresponds to negligible Spin-Orbit induced precession of periastron, while Wex & Kopeikin and this paper both found significant (but not equivalent) effects. The observational data of two typical binary pulsars, PSR J2051–0827 and PSR J1713+0747, apparently support a significant Spin-Orbit coupling effect. Specific binary pulsars with orbital plane nearly edge on could discriminate between Wex & Kopeikin and this paper: if the orbital period derivative of the double-pulsar system PSRs J0737–3039 A and B, with orbital inclination angle $i = 87.7^{+17}_{-29}$ deg, is much larger than that of the gravitational radiation induced one, then the expression in this paper is supported, otherwise Wex & Kopeikin's is supported.

**Key words:** pulsars: binary pulsars – geodetic precession: individual (PSR J2051–0827, PSR J1713+0747, PSRs J0737–3039 A and B)

## 1 INTRODUCTION

In the gravitational two-body problem with spin, each body is precessing in the gravitational field of its companion, with precession velocity of first order Post-Newtonian (PN) (Barker & O'Connell 1975, hereafter BO). This precession velocity is widely accepted. However, as to how the orbital plane reacts to the torque caused by the precession of the two bodies there are two approaches. In BO, the orbital precession velocity is obtained by assuming that the angular momentum vector, $\boldsymbol{L}$, precesses at the same velocity as the Runge-Lenz vector, $\boldsymbol{A}$. On the other hand, in the study of modulation of gravitational wave by Spin-Orbit (S-L) coupling effect in merging binaries, Apostolatos et al. (1994) and Kidder (1995) (hereafter AK) obtained an orbital precession velocity that satisfies the conservation of the total angular momentum, $\boldsymbol{J}$, and the triangle constraint, $\boldsymbol{J} = \boldsymbol{L} + \boldsymbol{S}$ (where $\boldsymbol{S}$ is the sum of spin angular momenta of

two bodies, $\boldsymbol{S}_1$ and $\boldsymbol{S}_2$). This difference in the assumptions leads to different physical behaviors between BO' and AK's orbital precession velocities. BO's expression is not consistent with the triangle constraint, whereas the AK's expression is. Moreover, the reason of this discrepancy is that the former actually assumes that the four vectors, $\boldsymbol{S}_1$, $\boldsymbol{S}_2$, $\boldsymbol{r}_1$ and $\boldsymbol{r}_2$ ($\boldsymbol{r}_1$, $\boldsymbol{r}_2$ being the position vectors of the two bodies), are independent; but, the latter assumes that the independent vectors are either $\boldsymbol{S}_1$, $\boldsymbol{r}_1$ and $\boldsymbol{r}_2$; or $\boldsymbol{S}_2$, $\boldsymbol{r}_1$ and $\boldsymbol{r}_2$.

The discrepancy between BO' and AK's precession velocities has an analogy in the following case. The motion of a small mass at the bottom of a clock pendulum can be described in the $x-y$ plane. However, if we treat the dimension of this case as 2, then the small mass can move freely in the 2-dimensional space, and the length of the pendulum is not a constant. In other words, once the length of the pendulum is a fixed constant, then the dimension is 1 instead of 2. Correspondingly if the free vectors of a binary system is 4, and the triangle constraint is not satisfied (or $\boldsymbol{J}$ cannot be a constant vector). On the other hand, if the triangle constraint is satisfied, the number of free vectors is 3, instead of 4.

In the application to pulsar timing measurement, BO's orbital precession velocity is treated in two different ways, by Damour & Schäfer (1988) and Wex & Kopeikin (1999) (hereafter WK), respectively. The former predicted an insignificant S-L coupling induced precession of periastron, $\dot{\omega}^S$, and hence an insignificant derivative of orbital period, $\dot{P}_b$; while the latter predicted a significant $\dot{\omega}^S$ and $\dot{P}_b$. In this paper we point out that the discrepancy is due to Damour & Schäfer and WK calculated the effects in two different coordinate systems. In the former, the coordinate system is not at rest to "an observer" at the Solar System Baryon center (SSB), whereas, in the latter, the coordinate system is at rest to the SSB. Relative to the SSB, the former coordinate system has a non-zero acceleration, but the latter has a zero acceleration.

We calculate the observational effect corresponding to AK's orbital precession velocity, which uses the same coordinate system as WK. Significant $\dot{\omega}^S$ and $\dot{P}_b$ are given, but they are not equivalent to the results given by WK. The validity of the two expressions can be tested by specific binary pulsars with orbital inclination close to $\pi/2$, i.e., the double-pulsar system PSRs J0737–3039 A and B.

This paper contains four parts: (a) the physical discrepancy between BO and AK's orbital precession velocity (Sections 2, 3); (b) the derivation of S-L coupling induced effect corresponding to AK's expression of orbital precession (Sections 4, 5, 9); (c) the discrepancy between the coordinate systems used by Damour & Schäfer (1988) and WK, as well as the relationships among three expressions for the S-L coupling induced effects, given by Damour & Schäfer, by WK and by this paper (Section 6); (d) confrontation of the three expressions based on the different S-L coupling models with observational data of PSR J2051–0827 and PSR J1713+0747, and different predictions on $\dot{\omega}^S$ and $\dot{P}_b$ of PSRs J0737–3039 A and B (Sections 7, 8).

## 2 ORBITAL PRECESSION VELOCITY

This section introduces the derivation of the orbital precession velocity of BO and AK.

### 2.1 Derivation of BO's Orbital Precession Velocity

BO's two-body equation was the first gravitational two-body equation with spin, it consists of two parts, the precession velocity of the spin angular momentum vectors of body one and body two, and the precession velocity of the and the orbital angular momentum vector. Body one precesses in the gravitational field of body two, with precession velocity (BO),

$$\dot{\boldsymbol{\Omega}}_1 = \frac{L(4+3m_2/m_1)}{2r^3}\,\hat{\boldsymbol{L}} + \frac{S_2}{2r^3}\left[\hat{\boldsymbol{S}}_2 - 3(\hat{\boldsymbol{L}}\cdot\hat{\boldsymbol{S}}_2)\,\hat{\boldsymbol{L}}\right], \tag{1}$$

where $\hat{\boldsymbol{L}}$, $\hat{\boldsymbol{S}}_1$ and $\hat{\boldsymbol{S}}_2$ are unit vectors of the orbital angular momentum, and of the spin angular momentum of star 1 and star 2, respectively. Here $\dot{\boldsymbol{\Omega}}_2$ can be obtained by exchanging the subscript 1 and 2 at the right side of Eq. (1). The first term of Eq. (1) represents the geodetic (de Sitter) precession, which corresponds to the precession of $\boldsymbol{S}_1$ around $\boldsymbol{L}$. It is 1PN due to $\frac{L}{r^3} \sim (\frac{v}{c})^2(\frac{v}{r})$. The second term represents the Lense-Thirring precession, $\boldsymbol{S}_1$ around $\boldsymbol{S}_2$, which is $\frac{S}{L}$ times smaller than the first. Therefore, it corresponds to 1.5PN. The precession velocity of the spin angular momentum vectors is confirmed by other authors using different methods. However, for the precession velocity of the orbit, there are different expressions. BO's orbital precession velocity is given as follows. The total Hamiltonian for the gravitational two-body problem with spin is given as (BO; Damour & Schäfer 1988)

$$H = H_{\rm N} + H_{\rm 1PN} + H_{\rm 2PN} + H_S \ , \tag{2}$$

where $H_{\rm N}$, $H_{\rm 1PN}$ and $H_{\rm 2PN}$ are the Newtonian, the first and second order post-Newtonian terms respectively. $H_{\rm S}$ is the spin-orbit interaction Hamiltonian (BO; Damour & Schäfer 1988),

$$H_{\rm S} = \sum_{\alpha=1}^{2} \Big(2 + 3\frac{m_{\alpha+1}}{m_\alpha}\Big)\Big(\frac{\boldsymbol{S}_\alpha \cdot \boldsymbol{L}}{r^3}\Big) \ , \tag{3}$$

where by $\alpha + 1$ is meant modulo 2 (2+1=1), $m_1$, $m_2$ are the masses of the two stars, $r = a(1-e^2)^{1/2}$, $a$ is the semi-major axis, $e$ is the eccentricity of the orbit. Note we use $G = c = 1$ units until Section 5 to Section 7 when we discuss observational effects .

The BO equation describes the secular effect on the orbital plane by a rotational velocity vector, $\dot{\Omega}_S$, acting on some instantaneous Newtonian ellipse. Damour & Schäfer (1988) computed $\dot{\Omega}_S$ in a simple manner by making full use of the Hamiltonian method. The functions of the canonically conjugate phase space variables $\boldsymbol{r}$ and $\boldsymbol{p}$ are defined as

$$\boldsymbol{L}(\boldsymbol{r}, \boldsymbol{p}) = \boldsymbol{r} \times \boldsymbol{p} \ , \tag{4}$$

$$\boldsymbol{A}(\boldsymbol{r}, \boldsymbol{p}) = \boldsymbol{p} \times \boldsymbol{L} - GM\mu^2 \frac{\boldsymbol{r}}{r} \ , \tag{5}$$

where $\boldsymbol{r} = \boldsymbol{r}_1 - \boldsymbol{r}_2$, $M = m_1 + m_2$, $\mu = m_1 m_2/M$. Vector $\boldsymbol{A}$ is the Runge-Lenz vector (first discovered by Lagrange). The instantaneous Newtonian ellipse evolves according to the fundamental equations of Hamiltonian dynamics (Damour & Schäfer 1988)

$$\dot{\boldsymbol{L}} = \{\boldsymbol{L}, H\} \ , \tag{6}$$

$$\dot{\boldsymbol{A}} = \{\boldsymbol{A}, H\} \ , \tag{7}$$

where $\{,\}$ denotes the Poisson bracket. $\boldsymbol{L}$ and $\boldsymbol{A}$ are first integrals of $H_{\rm N}$, only $H_{\rm 1PN}+H_{\rm 2PN}+H_{\rm S}$ contributes to the right-hand sides of Eqs. (6) and (7), in which $H_{\rm 1PN} + H_{\rm 2PN}$ determines the precession of periastron, in 1PN it is given as,

$$\dot{\omega}^{\rm GR} = \frac{6\pi M}{P_b a(1-e^2)} \ , \tag{8}$$

where $P_b$ is the orbital period. To study the spin-orbit interaction, it is sufficient to consider $H_{\rm S}$. Thus replacing $H$ of Eqs. (6) and (7) by $H_S$ one obtains (Damour & Schäfer 1988),

$$\Big(\frac{d\boldsymbol{L}}{dt}\Big)_{\rm S} = \{\boldsymbol{L}, H_{\rm S}\} = \dot{\Omega}_S^* \hat{\boldsymbol{S}} \times \boldsymbol{L} \ , \tag{9}$$

$$\Big(\frac{d\boldsymbol{A}}{dt}\Big)_S = \{\boldsymbol{A}, H_{\rm S}\} = \dot{\Omega}_S^* [\hat{\boldsymbol{S}} - 3(\hat{\boldsymbol{L}} \cdot \hat{\boldsymbol{S}})\hat{\boldsymbol{L}}] \times \boldsymbol{A} \ , \tag{10}$$

where

$$\dot{\Omega}_S^* = \frac{S(4+3m_2/m_1)}{2r^3} \ . \tag{11}$$

By Damour & Schäfer (1988), $\boldsymbol{S}$ represents a linear combination of $\boldsymbol{S}_1$ and $\boldsymbol{S}_2$. For simplicity and consistency with WK's application of $\dot{\boldsymbol{\Omega}}_S$, we assume $\boldsymbol{S} = \boldsymbol{S}_1$ (the other spin angular momentum is ignored) until Section 4 where the general binary pulsar is discussed.

The solution of Eqs. (9) and (10) gives the S-L coupling induced orbital precession velocity (Damour & Schäfer 1988)

$$\dot{\boldsymbol{\Omega}}_S = \dot{\Omega}_S^*[\hat{\boldsymbol{S}} - 3(\hat{\boldsymbol{L}}\cdot\hat{\boldsymbol{S}})\hat{\boldsymbol{L}}] \, . \tag{12}$$

By Eqs. (9) and (12), the first derivative of $\hat{\boldsymbol{L}}$ can be obtained

$$\frac{d\hat{\boldsymbol{L}}}{dt} = \dot{\Omega}_S^* \hat{\boldsymbol{S}} \times \hat{\boldsymbol{L}} \ , \tag{13}$$

and by Eq. (1) the first derivative of $\hat{\boldsymbol{S}}$ (recall $\boldsymbol{S} = \boldsymbol{S}_1$) can be written

$$\frac{d\hat{\boldsymbol{S}}}{dt} = \dot{\Omega}_1^* \hat{\boldsymbol{L}} \times \hat{\boldsymbol{S}} = \Omega_S^* \frac{L}{S} \hat{\boldsymbol{L}} \times \hat{\boldsymbol{S}} \ , \tag{14}$$

where $\dot{\Omega}_1^*$ is the first term at the right hand side of Eq. (1). By Eqs. (13) and (14) $\hat{\boldsymbol{L}}$ precesses slowly around $\hat{\boldsymbol{S}}$, 1.5PN, as shown by Eq. (13); but $\hat{\boldsymbol{S}}$ precesses rapidly around $\hat{\boldsymbol{L}}$, 1PN, as shown in Eq. (14). Therefore the BO's equation predicts a scenario in which the two vectors, $\hat{\boldsymbol{L}}$ and $\hat{\boldsymbol{S}}$ precess around each with very different precession velocities (typically one is larger than the other by 3 to 4 orders of magnitude for a general binary pulsar system).

### 2.2 Orbital Precession Velocity in the Calculation of Gravitational Waves

In the study of modulation of precession of orbital plane by gravitational waves, the orbital precession velocity is obtained in a different manner and the result is very different from that given by Eq. (12). Since the gravitational wave corresponds to 2.5PN, it is negligible compared to the S-L coupling effect that corresponds to 1PN and 1.5PN, and the total angular momentum can be treated as conserved, $\dot{\boldsymbol{J}} = 0$. Then the following equation can be obtained (BO),

$$\dot{\boldsymbol{\Omega}}_0 \times \boldsymbol{L} = -\dot{\boldsymbol{\Omega}}_1 \times \boldsymbol{S}_1 - \dot{\boldsymbol{\Omega}}_2 \times \boldsymbol{S}_2 \ . \tag{15}$$

Note that as defined by BO and AK, $\boldsymbol{L} = \mu M^{1/2} r^{1/2} \hat{\boldsymbol{L}}$. In the one-spin case the right side of Eq. (15) can be given as (Kidder 1995)

$$\dot{\boldsymbol{S}} = \frac{1}{2r^3}\Big(4 + \frac{3m_2}{m_1}\Big)(\boldsymbol{L} \times \boldsymbol{S}) \, , \tag{16}$$

and considering that $\boldsymbol{J} = \boldsymbol{L} + \boldsymbol{S}$, Eq. (16) can be written

$$\dot{\boldsymbol{S}} = \frac{1}{2r^3}\Big(4 + \frac{3m_2}{m_1}\Big)(\boldsymbol{J} \times \boldsymbol{S}) \ . \tag{17}$$

From Eq. (15), $\dot{\boldsymbol{L}}$ can be given

$$\dot{\boldsymbol{L}} = \frac{1}{2r^3}\Big(4 + \frac{3m_2}{m_1}\Big)(\boldsymbol{J} \times \boldsymbol{L}) \ . \tag{18}$$

By Eqs. (17) and (18), $\boldsymbol{L}$ and $\boldsymbol{S}$ precess about the fixed vector $\boldsymbol{J}$ at the same rate with a precession frequency approximately (AK)

$$\dot{\boldsymbol{\Omega}}_0 = \frac{\boldsymbol{J}}{2r^3}\Big(4 + \frac{3m_2}{m_1}\Big) \ . \tag{19}$$

Equation (19) indicates that in the 1PN approximation, $\hat{\boldsymbol{L}}$ and $\hat{\boldsymbol{S}}$ can precess around $\boldsymbol{J}$ rapidly (1PN) with exactly the same velocity. Note that the misalignment angles between $\hat{\boldsymbol{L}}$ and $\hat{\boldsymbol{S}}$ ($\lambda_{LS}$), $\hat{\boldsymbol{L}}$ and $\hat{\boldsymbol{J}}$ ($\lambda_{LJ}$) are very different, due to $S/L \ll 1$ , $\lambda_{LJ}$ is much smaller than $\lambda_{LS}$.

Thus, AK's equations, Eqs. (18) and (17), give a very different scenario of motion of $\boldsymbol{S}$, $\boldsymbol{L}$ and $\boldsymbol{J}$ from that given by BO equation shown in Eqs. (13) and (14).

## 3 PHYSICAL DIFFERENCES BETWEEN BO AND AK

This section compares the two different scenarios corresponding to BO' and AK's orbital precession velocity, and points out that BO's orbital precession velocity is actually inconsistent with the definition of the total angular momentum of a binary system.

Section 2 indicates that BO and AK derived the orbital precession velocity in different ways, therefore two different orbital precession velocity vectors were obtained, as shown in Eqs. (12) and (19), respectively, which in turn correspond to different scenarios of motion of the three vectors. This section shows that the discrepancy between BO and AK is not just a discrepancy due to different coordinate systems: actually there is a significant physical difference between BO and AK. In BO, the total angular momentum of a binary system is defined as

$$\boldsymbol{J} = \boldsymbol{L} + \boldsymbol{S} \ , \tag{20}$$

Eq. (20) means that $\boldsymbol{J}$, $\boldsymbol{L}$ and $\boldsymbol{S}$ form a triangle, and therefore, it guarantees that the three vectors must be in one plane at any moment. For a general radio binary pulsar system, the total angular momentum of this system is conserved in 1PN. Therefore we have

$$\dot{\boldsymbol{J}} = 0 \ . \tag{21}$$

Equation (21) means that $\boldsymbol{J}$ is a constant during the motion of a binary system. Equations (20) and (21) together provide a scenario in which the triangle formed by $\boldsymbol{L}$, $\boldsymbol{S}$ and $\boldsymbol{J}$ determines a plane, and the plane rotates around a fixed axis, $\boldsymbol{J}$, with velocity $\dot{\Omega}_0$. This scenario is shown in Fig. 1, which can also be represented as

$$\dot{\boldsymbol{J}} = \dot{\Omega}_0 \hat{\boldsymbol{J}} \times \boldsymbol{L} + \dot{\Omega}_0 \hat{\boldsymbol{J}} \times \boldsymbol{S} = 0 \, . \tag{22}$$

Smarr & Blandford (1976) mentioned the scenario that $\boldsymbol{L}$ and $\boldsymbol{S}$ must be at opposite sides of $\boldsymbol{J}$ at any instant. Hamilton & Sarazin (1982) also studied the scenario and stated that $\boldsymbol{L}$ precesses rapidly around $\boldsymbol{J}$. Obviously the orbital precession velocity given by Eq. (19) can satisfy the two constraints, Eqs. (20) and (21) simultaneously.

Can the BO's orbital precession velocity given by Eq. (12) satisfy the two constraints, Eqs. (20) and (21) simultaneously? From Eqs. (12), (13) and (14), the first derivative of $\boldsymbol{J}$ can be written (BO)

$$\dot{\boldsymbol{J}} = \dot{\boldsymbol{\Omega}}_S \times \boldsymbol{L} + \dot{\boldsymbol{\Omega}}_1^* \times \boldsymbol{S} = \dot{\Omega}_S^* \hat{\boldsymbol{S}} \times \boldsymbol{L} + \dot{\Omega}_1^* \hat{\boldsymbol{L}} \times \boldsymbol{S} \equiv 0 \ , \tag{23}$$

and since Eq. (20) is defined in BO's equation, then it seems that the BO equation can satisfy both Eqs. (20) and (21).

However, in BO's derivation of $\dot{\boldsymbol{\Omega}}_S$ (Eqs. (6)–(12)), Eq. (20) is never used. The corresponding $\dot{\boldsymbol{\Omega}}_S$ can make $\dot{\boldsymbol{J}} = \dot{\boldsymbol{L}} + \dot{\boldsymbol{S}} \equiv 0$, as shown in Eq. (23), but it cannot guarantee that $\boldsymbol{J} = \boldsymbol{L} + \boldsymbol{S}$ is satisfied. In other words, when $\boldsymbol{J} \neq \boldsymbol{L} + \boldsymbol{S}$, Eq. (23) is still correct. This can be easily tested by putting $\boldsymbol{L}' = \boldsymbol{L} + \alpha \boldsymbol{S}$, or $\boldsymbol{S}' = \boldsymbol{S} + \beta \boldsymbol{L}$ ($\alpha$ and $\beta$ are arbitrary constants) into Eq. (23) to replace $\boldsymbol{L}$ and $\boldsymbol{S}$, respectively. Obviously in such cases, Eq. (23) is still satisfied ($\dot{\boldsymbol{J}} \equiv 0$).

On the other hand, in AK's derivation of $\dot{\boldsymbol{\Omega}}_0$(Eqs. (16)–(18)), the relation Eq. (20) is used. If we do the same replacement of $\boldsymbol{L}' = \boldsymbol{L} + \alpha \boldsymbol{S}$, or $\boldsymbol{S}' = \boldsymbol{S} + \beta \boldsymbol{L}$ in Eq. (22), then Eq. (22) is

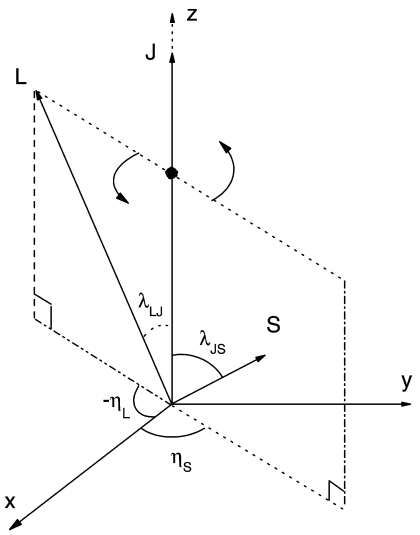


**Fig. 1** In 1PN, the scenario of motion of a binary pulsar system can be described as the rotation of the plane determined by $\boldsymbol{L}$, $\boldsymbol{S}$ around the fixed axis, $\boldsymbol{J}$. Here $\eta_L$ and $\eta_S$ are precession phases of $\boldsymbol{L}$ and $\boldsymbol{S}$ in the J-coordinate system, respectively.

violated ($\dot{\boldsymbol{J}} \neq 0$). This means that for AK's $\dot{\boldsymbol{\Omega}}_0$, if Eq. (20) is violated then Eq. (21) is violated also. Thus in AK's expression, the conservation of the total angular momentum is dependent on Eq. (20), whereas, in BO's expression, the conservation of the total angular momentum is independent of Eq. (20). If we rewrite Eq. (20) as

$$\boldsymbol{J} = \boldsymbol{L} + \boldsymbol{S} + \boldsymbol{C} \ , \tag{24}$$

then in BO's expression the conservation of the total angular momentum can be satisfied in the case that $\boldsymbol{C} \neq 0$ in Eq. (24); but, in AK's expression the conservation of the total angular momentum is satisfied only when $\boldsymbol{C} = 0$ in Eq. (24). This means that the discrepancy between BO and AK's orbital precession velocity is physical. It is not just a matter of different expressions in different coordinate systems or relative to different directions.

Moreover, Eqs. (22) and (19) correspond to the following orbital precession velocity,

$$\dot{\boldsymbol{\Omega}}_0 = \dot{\Omega}^*_S \Big( \hat{\boldsymbol{S}} + \frac{L}{S} \hat{\boldsymbol{L}} \Big) \, . \tag{25}$$

Obviously Eq. (25) is not consistent with BO's Eq. (12), which demands that the coefficient of the component along $\hat{\boldsymbol{L}}$ be $\gamma = -3(\hat{\boldsymbol{L}} \cdot \hat{\boldsymbol{S}})$, instead of $\gamma = \frac{L}{S}$ as given by Eq. (25).

In other words, once Eq. (20) is satisfied, BO's orbital precession velocity of Eq. (12) must be violated. Therefore, BO's orbital precession velocity cannot be consistent with BO's definition, $\boldsymbol{J} = \boldsymbol{L} + \boldsymbol{S}$. Actually Eq. (25) can be consistent with Eq. (9), however, it contradicts Eq. (10). The reason of introducing Eq. (10) is that without it Eq. (9) alone cannot determine a unique solution. However, Eqs. (22) and (19) can be regarded as solving this problem by using Eqs. (9) and (20) instead of Eqs. (9) and (10) to obtain the orbital precession velocity.

As defined in Eqs. (4) and (5), $\boldsymbol{L}$ and $\boldsymbol{A}$ are vectors that are determined by different elements in celestial mechanics, $\boldsymbol{L}(\Omega, i)$ and $\boldsymbol{A}(\Omega, i, \omega, e)$, respectively. These two vectors satisfy

different physical constraints, i.e., $\boldsymbol{L}$ satisfies Eqs. (20) and (21), but $\boldsymbol{A}$ does not satisfy these two constraints.

Therefore, it is conceivable that $\boldsymbol{L}$ and $\boldsymbol{A}$ should correspond to different precession velocities, as given by Eqs. (9) and (10), respectively. However, since the discrepancy is only in the $\hat{\boldsymbol{L}}$ component, which does not influence the satisfaction of the conservation equation, Eq. (23), the discrepancy seems unimportant. Therefore, the precession velocity of $\boldsymbol{L}$ is treated equivalently to that of $\boldsymbol{A}$'s, thus the components in $\hat{\boldsymbol{L}}$ are both treated as $\gamma = -3(\hat{\boldsymbol{L}} \cdot \hat{\boldsymbol{S}})$. However, as given by Eq. (25), $\hat{\boldsymbol{L}}$ component must be $\gamma = \frac{L}{S}$ if the triangle constraint is to be satisfied. Hence, the violation of the triangle constraint is inevitable under the assumption that $\boldsymbol{L}$ and $\boldsymbol{A}$ precess at the same velocity.

## 4 S-L COUPLING INDUCED EFFECTS DERIVED UNDER DIFFERENT DEGREES OF FREEDOM

As analyzed in Sections 2 and 3, the orbital precession velocity is dependent on the physical constraint imposed, on whether or not the triangle constraint is satisfied. This section further shows that the violation or satisfaction of the triangle constraint is due to different degrees of freedom used by BO and AK. To discuss the S-L coupling induced effects on the observational parameters, one needs to obtain the variation of the six orbital elements under S-L coupling. The way of doing this is to start from the Hamiltonian equation of motion (corresponding to S-L coupling), then through some perturbation method in celestial mechanics to obtain the S-L coupling induced variation of the six orbital elements, and finally transform the effects to the observer's coordinate system. In this section this process is performed in the case in which the triangle constraint is satisfied and the number of free vectors of a binary system (with two spins) is 3.

It is convenient to study the motion of a binary system in such a coordinate system (J-coordinate system), in which the total angular momentum $\boldsymbol{J}$ is along the z-axes and the invariance plane is the x-y plane. The J-coordinate system has two advantages:

(a) Once a binary pulsar system is given, $\lambda_{LJ}$, the misalignment angle between $\boldsymbol{J}$ and $\boldsymbol{L}$, can be estimated, from which $\dot{\Omega}$ and $\dot{\omega}$ can be obtained easily and are intrinsic to the binary pulsar system.

(b) The J-coordinate system is static relative to the line of sight (after leaving out the proper motion). Therefore, transforming the parameters obtained in the J-coordinates system to observer's coordinate system, S-L coupling induced effects can be reliably obtained. From Eq. (3), the S-L coupling induced $H_S$ contains only the potential part, therefore we have $H_S = U$, where

$$U = U_1 + U_2 = \frac{1}{r^3}\Big(2\boldsymbol{S} + \frac{3m_2}{2m_1}\boldsymbol{S}_1 + \frac{3m_1}{2m_2}\boldsymbol{S}_2\Big) \cdot \boldsymbol{L} \ , \tag{26}$$

which can be written as

$$U = \frac{1}{r^3}(\sigma_1 \boldsymbol{S} \cdot \boldsymbol{L} + \sigma_2 \boldsymbol{S}_2 \cdot \boldsymbol{L}) \ , \tag{27}$$

where

$$\sigma_1 = 2 + \frac{3}{2}\frac{m_2}{m_1} \quad , \quad \sigma_2 = 2 + \frac{3}{2}\Big(\frac{m_1}{m_2} - \frac{m_2}{m_1}\Big) \quad . \tag{28}$$

From Eq. (27) we have the Lagrangian corresponding to S-L coupling, $\Im = -U$. The Lagrange equation is

$$\frac{d}{dt}\Big(\frac{\partial \Im}{\partial \dot{q}_\kappa}\Big) - \frac{\partial \Im}{\partial q_\kappa} = 0 \quad , \quad (\kappa = 1, 2, ..., \beta) \tag{29}$$

where $q_\kappa$ is the generalized coordinate ($\beta$ is the number of degrees of freedom), given by $r_1^{(\alpha)}$, $r_2^{(\alpha)}$, $s_1^{(\alpha)}$, $s_2^{(\alpha)}$ $(\alpha = 1, 2, 3)$ representing, respectively, the position of body 1 and body 2; the

direction of the spin angular momentum of body 1 and body 2. Considering that $\boldsymbol{S}_1$ and $\boldsymbol{S}_2$ can vary in direction only, the $\alpha$ of $s_1^{(\alpha)}$, $s_2^{(\alpha)}$ is given $\alpha = 1, 2$.

Since the times scale of spin down of a pulsar in a binary pulsar system is much longer than that of the period of geodetic precession, the magnitude of $\boldsymbol{S}_1$ and $\boldsymbol{S}_2$ can be treated as constant (these two vectors can only vary in direction). However, since the misalignment angle between $\boldsymbol{S}_1$ and $\boldsymbol{L}$ ($\lambda_{LS1}$), as well as between $\boldsymbol{S}_2$ and $\boldsymbol{L}$ ($\lambda_{LS2}$), are also constants in BO's gravitational two-body equation (Barker & O'Connell 1975), we have $\partial(\boldsymbol{S}_1 \cdot \boldsymbol{L})/\partial s_1^{(\alpha)} = 0$ and $\partial(\boldsymbol{S}_2 \cdot \boldsymbol{L})/\partial s_2^{(\alpha)} = 0$. Thus we have $\partial\Im/\partial q_\kappa = 0$ for $q_\kappa = s_1^{(\alpha)}, s_2^{(\alpha)}$. Furthermore, since $\dot{\boldsymbol{S}}_1$ and $\dot{\boldsymbol{S}}_2$ do not appear in the Lagrangian $\Im$, we have $d(\partial\Im/\partial\dot{q}_\kappa)/dt = 0$ for $q_\kappa = s_1^{(\alpha)}, s_2^{(\alpha)}$. Therefore, we only need to calculate $d(\partial\Im/\partial\dot{q}_\kappa)/dt$ and $\partial\Im/\partial q_\kappa$ of Eq. (29) in the case where $q_\kappa = r_1^{(\alpha)}, r_2^{(\alpha)}$. The first term on the left side of Eq. (29) corresponds to a generalized force, which can be written as $d(\partial\Im/\partial\dot{q}_\kappa)/dt = F = \mu a_{so}$; and the second term is $\partial\Im/\partial q_\kappa = -\nabla U$ (where $\nabla$ represents gradient). Thus Eq. (29) can be rewritten

$$\boldsymbol{a}_{so} = -\frac{1}{\mu}\nabla U = -\frac{1}{\mu}\Big[\sigma_1 \nabla \frac{(\boldsymbol{S}\cdot\boldsymbol{L})}{r^3} + \sigma_2 \nabla \frac{(\boldsymbol{S}_2\cdot\boldsymbol{L})}{r^3}\Big] \quad . \tag{30}$$

The triangle constraint given by Eq. (20) indicates that $\boldsymbol{S}$ and $\boldsymbol{L}$ are not independent. Therefore, we cannot treat as free variables of Eq. (30), $r_1^{(\alpha)}$, $r_2^{(\alpha)}$, $s_1^{(\alpha)}$ and $s_2^{(\alpha)}$.

Classical mechanics shows us that constraints reduce the number of dimensions of a dynamic system. The geometric constraint $\boldsymbol{J} = \boldsymbol{L} + \boldsymbol{S}$ can be imposed on Eq. (30) through the replacement, $\boldsymbol{S} = \boldsymbol{J} - \boldsymbol{L}$. Thus the set of free variables in Eq. (30) is either $r_1^{(\alpha)}$, $r_2^{(\alpha)}$, and $s_1^{(\alpha)}$; or $r_1^{(\alpha)}$, $r_2^{(\alpha)}$, and $s_2^{(\alpha)}$ (depending on the definition of $\sigma_1$ and $\sigma_2$ in Eq. (28)). Therefore, replacing $\boldsymbol{S} = \boldsymbol{J} - \boldsymbol{L}$ in Eq. (30) means that the triangle constraint is imposed on the motion of binary system, and the number of dimensions are reduced from 10 to 8.

This is analogous to the calculation of the equation of motion of a simple clock pendulum. The motion of a small mass at the bottom of a clock pendulum can be described in the $x - y$ plane. However, if we treat the dimension of this small mass as 2, then this small mass can move freely in the 2-dimensional space, and the length of the pendulum is not a constant. In other words, once the length of the pendulum is fixed, the dimension is 1 instead of 2. Correspondingly if the dimension of a binary system is 10, then the satisfaction of the triangle constraint cannot be guaranteed (or $\boldsymbol{J}$=const vector cannot be guaranteed). Contrarily, if the triangle constraint is satisfied, the dimension is 8 instead of 10. By the replacement, $\boldsymbol{S} = \boldsymbol{J} - \boldsymbol{L}$, Eq. (30) can be re-written

$$\nabla\frac{(\boldsymbol{S}\cdot\boldsymbol{L})}{r^3} = \nabla\frac{[(\boldsymbol{J}-\boldsymbol{L})\cdot\boldsymbol{L}]}{r^3} = \nabla\frac{(\boldsymbol{J}\cdot\boldsymbol{L})}{r^3} - \nabla\frac{(\boldsymbol{L}\cdot\boldsymbol{L})}{r^3} \quad , \tag{31}$$

where $\boldsymbol{V}$ is the velocity of the reduced mass. By Eqs. (31) and (30), we have

$$\boldsymbol{a}_{so} = \frac{3}{r^3}[\sigma_1(\boldsymbol{J}-\boldsymbol{L})\cdot(\hat{\boldsymbol{n}}\times\boldsymbol{V})\hat{\boldsymbol{n}} + \sigma_2\boldsymbol{S}_2\cdot(\hat{\boldsymbol{n}}\times\boldsymbol{V})\hat{\boldsymbol{n}}]$$

$$+\frac{1}{r^3}[\sigma_1(\boldsymbol{V}\times\boldsymbol{J}) - 2\sigma_1(\boldsymbol{V}\times(\boldsymbol{J}-\boldsymbol{L})) - \sigma_2(\boldsymbol{V}\times\boldsymbol{S}_2)]\,, \tag{32}$$

where $\hat{\boldsymbol{n}}$ is the unit vector of $\boldsymbol{r}$. Replacing $\boldsymbol{J} - \boldsymbol{L}$ by $\boldsymbol{S}$, Eq. (32) can be written as

$$\boldsymbol{a}_{so} = \frac{3}{r^3}[\sigma_1\boldsymbol{S}\cdot(\hat{\boldsymbol{n}}\times\boldsymbol{V})\hat{\boldsymbol{n}} + \sigma_2\boldsymbol{S}_2\cdot(\hat{\boldsymbol{n}}\times\boldsymbol{V})\hat{\boldsymbol{n}}]$$

$$+\frac{1}{r^3}[\sigma_1(\boldsymbol{V}\times\boldsymbol{J}) - 2\sigma_1(\boldsymbol{V}\times\boldsymbol{S}) - \sigma_2(\boldsymbol{V}\times\boldsymbol{S}_2)]\,. \tag{33}$$

If one calculates $\boldsymbol{a}_{so}$ directly by Eq. (30) without imposing the triangle constraint, then the result can be given by replacing $\boldsymbol{J}$ of Eq. (33) by $\boldsymbol{S}$,

$$\boldsymbol{a}'_{so} = \frac{3}{r^3}[\sigma_1 \boldsymbol{S}\cdot(\hat{\boldsymbol{n}}\times\boldsymbol{V})\hat{\boldsymbol{n}} + \sigma_2 \boldsymbol{S}_2\cdot(\hat{\boldsymbol{n}}\times\boldsymbol{V})\hat{\boldsymbol{n}}]$$

$$+\frac{2}{r^3}[\sigma_1(\boldsymbol{V}\times\boldsymbol{S}) + \sigma_2(\boldsymbol{V}\times\boldsymbol{S}_2)]$$

$$+\frac{3(\boldsymbol{V}\cdot\hat{\boldsymbol{n}})}{r^3}[\sigma_1(\boldsymbol{S}\times\hat{\boldsymbol{n}}) + \sigma_2(\boldsymbol{S}_2\times\hat{\boldsymbol{n}})] \ . \tag{34}$$

The difference between Eqs. (33) and (34) indicates that whether the triangle constraint is satisfied or can not lead to significant differences in $\boldsymbol{a}_{so}$, which in turn results in significant differences on the predictions of observational effects as the next section will show.

Having obtained $\boldsymbol{a}_{so}$, we can use the standard method in celestial mechanics to calculate

$$\widetilde{S} = \boldsymbol{a}_{so}\cdot\hat{\boldsymbol{n}}, \quad \widetilde{T} = \boldsymbol{a}_{so}\cdot\hat{\boldsymbol{t}}, \quad \widetilde{W} = \boldsymbol{a}_{so}\cdot\hat{\boldsymbol{L}}, \tag{35}$$

from which we can calculate the derivative of the six orbit elements and then transform these to the observer's coordinate system to compare with the observations. The unit vectors, $\hat{\boldsymbol{n}}$, in Eqs. (33)–(35) are given by

$$\hat{\boldsymbol{n}} = \boldsymbol{P}\cos f + \boldsymbol{Q}\sin f \ , \tag{36}$$

and $\hat{\boldsymbol{t}}$ is the unit vector that is perpendicular to $\hat{\boldsymbol{n}}$,

$$\hat{\boldsymbol{t}} = -\boldsymbol{P}\sin f + \boldsymbol{Q}\cos f \ , \tag{37}$$

$\boldsymbol{V} = \boldsymbol{p}/\mu$, is given by

$$\boldsymbol{V} = -\frac{h}{p}\boldsymbol{P}\sin f + \frac{h}{p}\boldsymbol{Q}(e+\cos f) \ , \tag{38}$$

where $f$ is the true anomaly, $p$ is the semi-latus rectum, $p = a(1-e^2)$, and $h$ is the integral of area, $h = r^2\dot{f}$. $\boldsymbol{P}$ has the three components,

$$P_x = \cos\Omega\cos\omega - \sin\Omega\sin\omega\cos\lambda_{LJ} \ ,$$

$$P_y = \sin\Omega\cos\omega + \cos\Omega\sin\omega\cos\lambda_{LJ} \ ,$$

$$P_z = \sin\omega\sin\lambda_{LJ} \ ; \tag{39}$$

and for $\boldsymbol{Q}$, the three components,

$$Q_x = -\cos\Omega\sin\omega - \sin\Omega\cos\omega\cos\lambda_{LJ} \ ,$$

$$Q_y = -\sin\Omega\sin\omega + \cos\Omega\cos\omega\cos\lambda_{LJ} \ ,$$

$$Q_z = \cos\omega\sin\lambda_{LJ} \ . \tag{40}$$

The unit vectors of $\hat{\boldsymbol{L}}$ and $\hat{\boldsymbol{S}}_\kappa$ ($\kappa = 1, 2$) are given by

$$\hat{\boldsymbol{L}} = (\sin\lambda_{LJ}\cos\eta_L, \ \sin\lambda_{LJ}\sin\eta_L, \ \cos\lambda_{LJ})^T \ , \tag{41}$$

$$\hat{\boldsymbol{S}}_\kappa = (\sin\lambda_{JS\kappa}\cos\eta_{S\kappa}, \ \sin\lambda_{JS\kappa}\sin\eta_{S\kappa}, \ \cos\lambda_{JS\kappa})^T \ . \tag{42}$$

In the perturbation equation, the acceleration of Eq. (33), $\boldsymbol{a}_{so}$, is expressed along $\hat{\boldsymbol{n}}$, $\hat{\boldsymbol{t}}$ and $\hat{\boldsymbol{L}}$ respectively. We can use $\boldsymbol{a}_1$ and $\boldsymbol{a}_2$ to represent terms corresponding to the two terms containing brackets $[,]$ at the right hand side of Eq. (33), respectively. Projecting $\boldsymbol{a}_1$ onto $\hat{\boldsymbol{L}}$, we have

$$W_1 = \boldsymbol{a}_1 \cdot \hat{\boldsymbol{L}} = \frac{3\sigma_1}{r^3}[S_x(n_yV_z - n_zV_y) + S_y(n_zV_x - n_xV_z) + S_z(n_zV_y - n_yV_z)]$$

$$(n_x \sin\lambda_{LJ}\cos\eta_L + n_y \sin\lambda_{LJ}\sin\eta_L + n_z\cos\lambda_{LJ}) \ , \tag{43}$$

where $n_x$, $n_y$, $n_z$ and $V(\alpha = 1, 2, 3)_x$, $V_y$, $V_z$ are the components of $\hat{\boldsymbol{n}}$ and $\boldsymbol{V}$ along axes, $x$, $y$ and $z$, respectively. Projecting $\boldsymbol{a}_2$ onto $\hat{\boldsymbol{L}}$, we have $W_2 = 0$. Therefore, the sum of $W$ is

$$\widetilde{W} = W_1 + W_2 = W_1 \ . \tag{44}$$

The effect around $\boldsymbol{J}$ can be obtained by the perturbation equations (Roy 1991; Yi 1993; Liu 1993) and Eq. (44)

$$\frac{d\Omega}{dt} = \frac{\widetilde{W} r\sin(\omega + f)}{na^2\sqrt{1-e^2}} \frac{1}{\sin\lambda_{LJ}} \ , \tag{45}$$

where $n$ is the angular velocity. Averaging over one orbital period we have

$$\left\langle \frac{d\Omega}{dt} \right\rangle = \frac{3\cos\lambda_{LJ}}{2a^3(1-e^2)^{3/2}\sin\lambda_{LJ}}(P_z\sin\omega + Q_x\cos\omega)[(P_yQ_z - P_zQ_y)(S_x\sigma_1 + S_{2x}\sigma_2)$$

$$+(P_zQ_x - P_xQ_z)(S_y\sigma_1 + S_{2y}\sigma_2) + (P_xQ_y - P_yQ_x)(S_z\sigma_1 + S_{2z}\sigma_2)] \ . \tag{46}$$

Note that the average value of Eq. (46) depends on $W_1$ only. With $S/\sin\lambda_{LJ} \sim L$, we have $d\Omega/dt \sim L/a^3$, which corresponds to 1PN.

The term $d\omega/dt$ can be obtained by calculation of $\widetilde{S} = \boldsymbol{a}_{so} \cdot \hat{\boldsymbol{n}}$ and $\widetilde{T} = \boldsymbol{a}_{so} \cdot \hat{\boldsymbol{t}}$. Since $\boldsymbol{a}_1 \cdot \hat{\boldsymbol{n}}$ and $\boldsymbol{a}_1 \cdot \hat{\boldsymbol{t}}$ are 1.5PN, it is sufficient to consider the projection of $\boldsymbol{a}_2$ onto $\hat{\boldsymbol{n}}$, $\hat{\boldsymbol{t}}$, respectively, thus we have

$$\left\langle (\boldsymbol{a}_2 \cdot \hat{\boldsymbol{n}})\cos f \right\rangle = \frac{7\sigma_1 J}{8(1-e^2)^{3/2}a^3}\frac{eh}{p}(P_xQ_y - P_yQ_x) \ , \tag{47}$$

$$\left\langle (\boldsymbol{a}_2 \cdot \hat{\boldsymbol{t}})\sin f \right\rangle = \frac{-5\sigma_1 J}{8(1-e^2)^{3/2}a^3}\frac{eh}{p}(P_xQ_y - P_yQ_x) \ . \tag{48}$$

From Eqs. (47) and (48), we have

$$\frac{d\omega'}{dt} = \frac{\sqrt{1-e^2}}{nae}\{[-\boldsymbol{a}_2 \cdot \hat{\boldsymbol{n}}]\cos f + (1 + \frac{r}{p})[\boldsymbol{a}_2 \cdot \hat{\boldsymbol{t}}]\sin f\}$$

$$= \frac{2\sigma_1 J}{(1-e^2)^{3/2}a^3}(P_yQ_x - P_xQ_y) \ . \tag{49}$$

Therefore, by the standard perturbation(Roy 1991; Yi 1993; Liu 1993), the advance of precession of periastron induced by S-L coupling is given by

$$\frac{d\omega}{dt} = \frac{d\omega'}{dt} - \frac{d\Omega}{dt}\cos\lambda_{LJ} \ . \tag{50}$$

By putting Eqs. (47) and (48) into Eq. (50), and averaging over one orbital period, we have

$$\left\langle \frac{d\omega}{dt} \right\rangle = \frac{2\sigma_1 J}{(1-e^2)^{3/2}a^3}(P_yQ_x - P_xQ_y) - \frac{d\Omega}{dt}\cos\lambda_{LJ} \ . \tag{51}$$

Using perturbation equations as in (Roy 1991; Yi 1993; Liu 1993), and by Eqs. (45) and (51), we have

$$\left\langle \frac{d\varpi}{dt} \right\rangle = \frac{2\sigma_1 J}{(1-e^2)^{3/2}a^3}(P_y Q_x - P_x Q_y) + 2\frac{d\Omega}{dt}\sin^2\frac{\lambda_{LJ}}{2}$$
$$= \frac{2\sigma_1 J}{(1-e^2)^{3/2}a^3}(P_y Q_x - P_x Q_y) + O(c^{-3}) \quad , \tag{52}$$

where $\varpi = \omega + \Omega$. Eqs. (46), (51) and (52) indicate that the magnitude of $d\Omega/dt$, and $d\varpi/dt$ are both $L/a^3$ (1PN).

In $d\Omega/dt$ (1PN) of Eq. (45) is equivalent to $\dot{\Phi}_S$ (1PN) which was given by WK. This is because the averaged value of $d\Omega/dt$ depends only on $\boldsymbol{a}_1$, the first term containing bracket [,] in $\boldsymbol{a}_{so}$, as shown in Eq. (33). Both this paper ($\boldsymbol{a}_{so}$, Eq. (33)), and the BO equation ($\boldsymbol{a}'_{so}$ of Eq. (34)) give the same $\boldsymbol{a}_1$. Thus, different authors give equivalent value on the averaged $d\Omega/dt$.

In contrast, $d\omega/dt$ of Eq. (51) and $\dot{\Psi}_S$ (1PN) given by WK are very different in magnitude. The difference is due to the fact that $d\omega/dt$ given by Eq. (51) is obtained by the $\boldsymbol{a}_{so}$ of Eq. (33); but the corresponding $d\omega/dt$ of WK is obtained by the $\boldsymbol{a}'_{so}$ of Eq. (34), which is equivalent of replacing $J$ of Eq. (33) by $S$.

In turn, the difference between $\boldsymbol{a}_{so}$ and $\boldsymbol{a}'_{so}$ is due to the fact that $\boldsymbol{a}_{so}$ satisfies the triangle constraint; but $\boldsymbol{a}'_{so}$ does not. Therefore, a small difference in the equation of motion causes significant discrepancy in the variation of elements, such as $d\omega/dt$.

## 5 EFFECTS ON $\dot{\omega}$, $\dot{X}$, $\dot{P}_b$

As shown in Section 4 the S-L coupling effect can be treated as a perturbation to the Newtonian two-body problem, and by the standard method in celestial mechanics the variation of six orbital elements can be obtained. This section calculates what $\dot{\omega}$, $\dot{x}$, $\dot{P}_b$ are for an observer when the variations of the six orbital elements are given. The results of this section are independent of the dimension used in a binary system.

The observational effect is studied in a coordinate system where the vector $\boldsymbol{K}_0$ (corresponding to line of sight) is along the $z'$-axis; the $x'$ axis is along the intersection of the plane of the sky and the invariance plane; and the $y'$-axis is perpendicular to $x'-z'$ plane, as shown in Fig. 2a. Obviously this coordinate system is at rest to "an observer" at the SSB. The relationship of the dynamical longitude of the ascending node, $\Omega$, the dynamical longitude of the periastron, $\omega$, and the orbital inclination, $i$, is given as (Smarr & Blandford 1976; WK)

$$\cos i = \cos I \cos\lambda_{LJ} - \sin\lambda_{LJ}\sin I\cos\Omega \quad , \tag{53}$$

and

$$\sin i \sin\omega^{\rm obs} = (\cos I\sin\lambda_{LJ} + \cos\lambda_{LJ}\sin I\cos\Omega)\sin\omega$$
$$+ \sin I\sin\Omega\cos\omega \quad , \tag{54}$$
$$\sin i\cos\omega^{\rm obs} = (\cos I\sin\lambda_{LJ} + \cos\lambda_{LJ}\sin I\cos\Omega)\cos\omega$$
$$- \sin I\sin\Omega\sin\omega \quad , \tag{55}$$

where $I$ is the misalignment angle between $\boldsymbol{J}$ and the line of sight. The semi-major axis of the pulsar is defined as

$$x \equiv \frac{a_p \sin i}{c} \quad , \tag{56}$$

where $a_p$ is the semi-major axis of the pulsar. By Eq. (53) we have

$$\dot{x}_1 = \frac{a_p\cos i}{c}\frac{di}{dt} = -x\dot{\Omega}\sin\lambda_{LJ}\sin\Omega\cot i \quad . \tag{57}$$

The semi-major axis of the orbit is $a = \frac{M}{m_2} a_p$, and since the L-S coupling induced $\dot{a}$ is a function of $\Omega$ and $\omega$, as shown in the appendix, we have

$$\dot{x}_2 = \frac{\dot{a}_p \sin i}{c} = \frac{\dot{a}}{a} x \ . \tag{58}$$

Therefore, the L-S coupling induced $\dot{x}$ is given by

$$\dot{x} = \dot{x}_1 + \dot{x}_2 = -x\dot{\Omega} \sin \lambda_{LJ} \sin \Omega \cot i + \frac{\dot{a}}{a} x \ . \tag{59}$$

By Eq. (59) we have

$$\ddot{x} = \dot{x}_1 \left( \frac{\ddot{\Omega}}{\dot{\Omega}} + \dot{\Omega} \cot \Omega + \frac{\dot{\lambda}_{LJ} \cos \lambda_{LJ}}{\sin \lambda_{LJ}} \right) + x \frac{\ddot{a}a - \dot{a}^2}{a^2} + \dot{x}_2 \frac{\dot{a}}{a} \ . \tag{60}$$

Note that $\dot{\Omega}$ and $\ddot{\Omega}$ can be obtained by Eq. (45). Considering $\lambda_{LJ} \ll 1$ and by Eqs. (54) and (55), the observational advance of precession of periastron is given (Smarr & Blandford 1976; WK),

$$\omega^{\rm obs} = \omega + \Omega - \lambda_{LJ} \cot i \sin \Omega \ . \tag{61}$$

Therefore, we have

$$\dot{\omega}^{\rm obs} = \dot{\omega} + \dot{\Omega} - \dot{\lambda}_{LJ} \cot i \sin \Omega \ . \tag{62}$$

If $\dot{\omega}$ and $\dot{\Omega}$ are caused only by the S-L coupling effect ($H = H_S$), then $\dot{\omega}$ is given by Eq. (51). If we consider all the terms of the Hamiltonian, as given by Eq. (2), then $\dot{\omega}$ should include $\dot{\omega}^{\rm GR}$, the advance of periastron predicted by general relativity, caused by $H_{\rm 1PN}$ and $H_{\rm 2PN}$. In this case $\dot{\omega}$ in Eq. (62) is replaced by $\dot{\omega}^{\rm GR} + \dot{\omega}$. Thus Eq. (62) can be written as

$$\dot{\omega}^{\rm obs} = \dot{\omega}^{\rm GR} + \dot{\omega}^S \ . \tag{63}$$

where

$$\dot{\omega}^S = \dot{\omega} + \dot{\Omega} - \dot{\lambda}_{LJ} \cot i \sin \Omega \ . \tag{64}$$

Note that $\dot{\omega}^S$ is a function of time due to $\dot{\Omega}$, $\dot{\omega}$ and $\dot{\lambda}_{LJ}$ are functions of time, as shown in Eqs. (46), (51) and ($A6$), respectively. While $\dot{\omega}^{\rm GR}$ is a constant as shown in Eq. (8).

For a binary pulsar system with negligibly small eccentricity, the effect of the variation in the advance of periastron, $\omega$, is absorbed by the redefinition of the orbital frequency. As discussed by Kopeikin (1996), $\omega^{\rm obs} + A_e(u)$ is given

$$\omega^{\rm obs} + A_e(u) = \omega_0 + \frac{2\pi}{P_b}(t - t_0) \ , \tag{65}$$

where $A_e(u)$ is the true anomaly, related to the eccentric anomaly, $u$, by the well-known transcendental equation, and $\omega_0$ is the orbital phase at the initial epoch $t_0$.

At the time interval, $\delta t = (t - t_0)$, there is a corresponding $\delta\omega^{\rm obs}$ which causes a corresponding $\delta P_b$ on the right hand side of Eq. (65). Therefore, $P_b$ is a function of time. Thus we have

$$\delta\omega^{\rm obs} + A_e(u) = \frac{2\pi}{P_b} \delta t \ . \tag{66}$$

Write $1/P_b$ in Taylor series, we have

$$\frac{1}{P_b} = \frac{1}{P_b(t_0)} - \frac{\dot{P}_b(t_0)\delta t}{P_b^2(t_0)} + ... \tag{67}$$

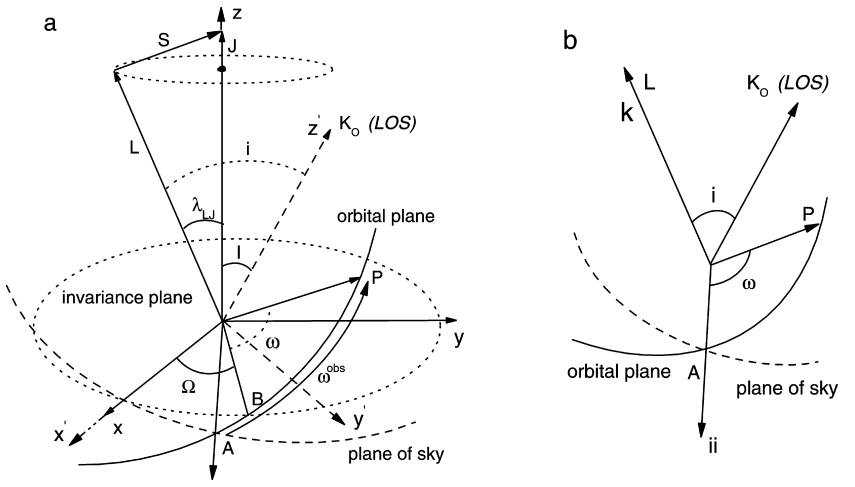


**Fig. 2** (a) Binary geometry and definitions of angles of Wex & Kopeikin (1999) and this paper. The invariable plane $(x - y)$, represented by the dotted ellipse, is perpendicular to the total angular momentum, $\boldsymbol{J}$. The inclination of the orbital plane with respect to the invariable plane is $\lambda_{LJ}$, which is also the precession cone angle of $\boldsymbol{L}$ around $\boldsymbol{J}$. The orbital inclination with respect to the line of sight is $i$, $\Omega$ is the longitude of the ascending node, $\omega$ is the longitude of the periastron from point B, and $\dot{\omega}^{\rm obs}$ is longitude of the periastron from point A. The J-coordinate system is defined by $(x, y, z)$, and the observer's coordinate system, by $(x', y', z')$. (b) Coordinate system of Damour & Schäfer (1988), which is determined by the triad $(\hat{\boldsymbol{L}}, \boldsymbol{i}, \boldsymbol{K}_0)$. Here ii represents $\boldsymbol{i}$.

Considering $A_e(u) = 2\pi\delta t/P_b(t_0)$ and by Eqs. (66) and (67) we obtain

$$\delta\dot{\omega}^{\rm obs} = -\frac{2\pi\dot{P}_b}{P_b^2}\delta t \ . \tag{68}$$

Since $\dot{\omega}^S$ is a function of time, and $\dot{\omega}^{\rm GR}$ =const, we have $\ddot{\omega}^{\rm obs} = \ddot{\omega}^S$ by Eq. (63). Assume $F = \dot{\omega}^S$, and write it in Taylor series as: $F = F_0 + \dot{F}\delta t + \frac{1}{2}\ddot{F}\delta t^2$, we obtain $\delta F = \delta\dot{\omega}^S \approx \dot{F}\delta t = \ddot{\omega}^S\delta t$. Therefore, $\delta\dot{\omega}^{\rm obs}$ of Eq. (68) becomes $\delta\dot{\omega}^S = \ddot{\omega}^S\delta t$, from which Eq. (68) can be written as

$$\dot{P}_b = -\frac{\ddot{\omega}^S P_b^2}{2\pi} \ . \tag{69}$$

By Eq. (69), the derivatives of $P_b$ can be obtained:

$$\ddot{P}_b = \frac{2\dot{P}_b^2}{P_b} - \frac{P_b^2}{2\pi}\frac{d^3\omega^S}{dt^3} \approx -\frac{P_b^2}{2\pi}\frac{d^3\omega^S}{dt^3} \, , \tag{70}$$

$$\frac{d^3P_b}{dt^3} \approx -\frac{P_b^2}{2\pi}\frac{d^4\omega^S}{dt^4} \, . \tag{71}$$

## 6 COMPARISON OF THREE DIFFERENT S-L COUPLING INDUCED $\dot{\omega}^{\rm obs}$ AND $\dot{P}_b$

### 6.1 Discrepancy between Wex & Kopeikin and this paper

Section 4 calculates the S-L coupling induced change of orbital elements of a binary system directly in the J-coordinate system (in which $z$ axis is along $\hat{\boldsymbol{J}}$ and $x-y$ plane is the invariance plane), and Section 5 transforms the effects in J-coordinate system to the observer's coordinate system, and obtains $\dot{x}$, $\dot{\omega}^{\rm obs}$ and $\dot{P}_b$. In which $\omega^{\rm obs}$ is equivalent to the definition of WK as shown in Fig. 2a.

By Eq. (51) the $\dot{\omega}$ can be 1.5PN (or $\dot{\omega}=0$ in 1PN), thus by Eq. (64) the S-L coupling induced precession of periastron, $\dot{\omega}^S$, becomes

$$\dot{\omega}^S \approx \dot{\varpi} - \dot{\lambda}_{LJ}\cot i \sin\Omega \ . \tag{72}$$

Equation (72) is the result corresponding to 8 degrees of freedom, and $\dot{\omega}^S$ is 1PN. On the other hand, WK rewrote BO's orbital precession velocity, Eq. (12) in the J-coordinate system, and then obtained $\dot{x}$, $\dot{\omega}^{\rm obs}$ in observer's coordinate system.

However, the difference is that for WK, all the results in the J-coordinate system are calculated in 10 dimensions. In this case $J$ in Eq. (51) is replaced by $S$, and hence the first term on the right side of Eq. (51) is 0.5PN smaller than that of the second term. Therefore, $\dot{\omega}$ can be represented by the second term on the right side of Eq. (51), which is 1PN. By Eq. (64) and by considering $\dot{\Omega}-\dot{\Omega}\cos\lambda_{LJ}\sim 1.5PN$ ($\lambda_{LJ}\ll 1$), we have

$$\dot{\omega}^S \approx -\dot{\lambda}_{LJ}\cot i \sin\Omega \ . \tag{73}$$

Although $\lambda_{LJ}\sim S/L\ll 1$, $\dot{\lambda}_{LJ}$ is significant, being 1PN ($\dot{\lambda}_{LJ}\sim\dot{\Omega}$), as shown in Eqs. (A5) and (A6). Consequently $\dot{\omega}^S$ is also 1PN, which leads to significant $\ddot{\omega}^S$ (1PN), and therefore, significant derivative of $P_b$ by Eqs. (69)–(71). In other words, WK's $\omega$ of Eq. (59) actually contains significant variabilities, such as $\dot{\omega}^S$ and $\dot{P}_b$, which seem to have been ignored.

Therefore, this paper and WK, which correspond to Eqs. (72) and(73) respectively, both predict significant $\dot{\omega}^S$ and $\dot{P}_b$. However, there is an obvious difference between them, namely, in Eq. (73), $\dot{\omega}^S\to 0$ when $i\to\pi/2$, but Eq. (72) does not have such a relation. Therefore, the validity of WK versus this paper can be tested by binary pulsar systems with orbital inclination, $i\to\pi/2$ (edge on).

If a binary pulsar system with $i\to\pi/2$ still has significant $\dot{P}_b$ (1PN), then Eq. (73) corresponding to WK is not supported; otherwise, Eq. (72) corresponding to this paper is not supported.

The discrepancy between Eqs. (72) and (73) is due to the discrepancy in $\dot{\omega}$, which is caused by the different number of dimensions used in this paper and in WK.

Equations (72) and (73) have an important property in common, namely, $\dot{\omega}^S$ (and therefore, $\dot{\omega}^{\rm obs}$) is obtained by the transformation from the J-coordinate system to the observer's coordinate system, in which all the three triads are at rest to SSB.

### 6.2 Discrepancy between Damour & Schäfer and Wex & Kopeikin

Damour & Schäfer (1988) expressed the orbital precession velocity as,

$$\dot{\boldsymbol{\Omega}}_S = \frac{d\Omega_S}{dt}\boldsymbol{K}_0 + \frac{d\omega}{dt}\boldsymbol{k} + \frac{di}{dt}\boldsymbol{i} \ , \tag{74}$$

where the $\boldsymbol{K}_0$ unit vector is along the line of sight, which defines the third vector of a reference triad ($\boldsymbol{I}_0$, $\boldsymbol{J}_0$, $\boldsymbol{K}_0$), where $\boldsymbol{I}_0$-$\boldsymbol{J}_0$ correspond to the plane of the sky. The triad of the orbit is ($\boldsymbol{i}$,

$\boldsymbol{j}$, $\boldsymbol{k}$), in which $\boldsymbol{k}$ corresponds to $\hat{\boldsymbol{L}}$, $\boldsymbol{i}$ is the nodal vector determined by the intersection of the two planes (note that it is different from the scalar, $i$, which represents the orbital inclination), as shown in Fig. 2b. By Eq. (74), and the relations between the reference triad, components of $\dot{\boldsymbol{\Omega}}_S$ are obtained (Damour & Schäfer 1988).

$$\frac{d\omega}{dt} = \frac{1}{\sin^2 i}[\dot{\boldsymbol{\Omega}}_S \cdot \boldsymbol{k} - \dot{\boldsymbol{\Omega}}_S \cdot \boldsymbol{K}_0 \cos i] \ , \tag{75}$$

$$\frac{d\Omega_S}{dt} = \frac{1}{\sin^2 i}[\dot{\boldsymbol{\Omega}}_S \cdot \boldsymbol{K}_0 - \dot{\boldsymbol{\Omega}}_S \cdot \boldsymbol{k} \cos i] \ , \tag{76}$$

$$\frac{di}{dt} = \dot{\boldsymbol{\Omega}}_S \cdot \boldsymbol{i} \ . \tag{77}$$

S-L coupling induced $\dot{\omega}$ given by Eq. (75) is $\dot{\omega} \sim \dot{\Omega}_S \sim$1.5PN. Therefore, Damour & Schäfer (1988) predicted an insignificant $\dot{\omega}$ ($\dot{\omega}^S$) much smaller than 1PN, and hence a correspondingly insignificant $\dot{P}_b$.

Thus it seems strange that Damour & Schäfer (1988) and WK while starting from the same orbital precession velocity given by Eq. (12), predicted a different observable effect. This is because $\dot{\omega}^S$ of WK is calculated in a coordinate system with the axes ($x'$, $y'$, $z'$) at rest to SSB as shown in Fig. 2a, but, $\dot{\omega}$ ($\dot{\omega}^S$) of Damour & Schäfer is calculated in the coordinate system with triad ($\boldsymbol{K}_0$, $\boldsymbol{k}$, $\boldsymbol{i}$), which is not at rest relative to SSB as shown in Fig. 2b. Obviously, $\boldsymbol{i}$ (point A), which is the intersection of the plane of the sky and the orbital plane of the binary system, is not static in the coordinate system ($x'$, $y'$, $z'$) of WK, and this applies also to $\boldsymbol{k}$. In other words, the triad ($\boldsymbol{K}_0$, $\boldsymbol{k}$, $\boldsymbol{i}$) has a non-zero acceleration relative to SSB. Therefore, effects calculated based on such triad cannot be directly compared with observations.

Obviously, if Damour & Schäfer's $\dot{\omega}$ was also calculated in the coordinate system as that of WK, then Eq. (75) reduces to Eq. (73). Thus, the discrepancy between Damour & Schäfer (1988) and WK is that the former calculated in a coordinate system which is not at rest to SSB while the latter, at rest to SSB. On the other hand, the discrepancy between WK and this paper is due to the different number of dimensions used in the calculation of the equation of motion of a binary system. The relationship of the three expressions of the S-L coupling effect is shown in Fig. 3 and Table 1.

**Table 1** Comparison of S-L coupling induced variabilities given by different authors

| | DS (1988) | WK (1999) | This paper | Evidence |
|---|---|---|---|---|
| $\dot{\Omega}$ in J-co | | 1PN | 1PN | |
| $\dot{\omega}$ in J-co | | 1PN | 1.5PN | |
| $\dot{\omega}^{\rm S}$ | $\sim \dot{\Omega}_S$ (of Eq. (12)) | $-\dot{\lambda}_{LJ} \cot i \sin \Omega$ | $\dot{\varpi} - \dot{\lambda}_{LJ} \cot i \sin \Omega$ | |
| $\dot{\omega}^{\rm obs}$ | $\dot{\omega}^{\rm GR}$+1.5PN | $\dot{\omega}^{\rm GR}$+1PN | $\dot{\omega}^{\rm GR}$+1PN | |
| $\dot{P}_b$ | $\dot{P}_b^{\rm GR}$ | $\lvert\dot{P}_b^{\rm obs}\rvert \gg \lvert\dot{P}_b^{\rm GR}\rvert$ | $\lvert\dot{P}_b^{\rm obs}\rvert \gg \lvert\dot{P}_b^{\rm GR}\rvert$ | $\lvert\dot{P}_b^{\rm obs}\rvert \gg \lvert\dot{P}_b^{\rm GR}\rvert$ |
| when $i \to \pi/2$ | | $\dot{P}_b^{\rm obs} \to \dot{P}_b^{\rm GR}$ | $\lvert\dot{P}_b^{\rm obs}\rvert \gg \lvert\dot{P}_b^{\rm GR}\rvert$ | |

J-co represents J-coordinate system, $\dot{P}_b^{\rm GR}$ represents orbital period change due to gravitational radiation predicted by General Relativity. $\dot{\Omega}_S$ is given by Eq. (12) which is 1.5PN, while $\dot{\Omega}$ and $\dot{\lambda}_{LJ}$ are 1PN, as given by Eqs. (46) and (A5), respectively.

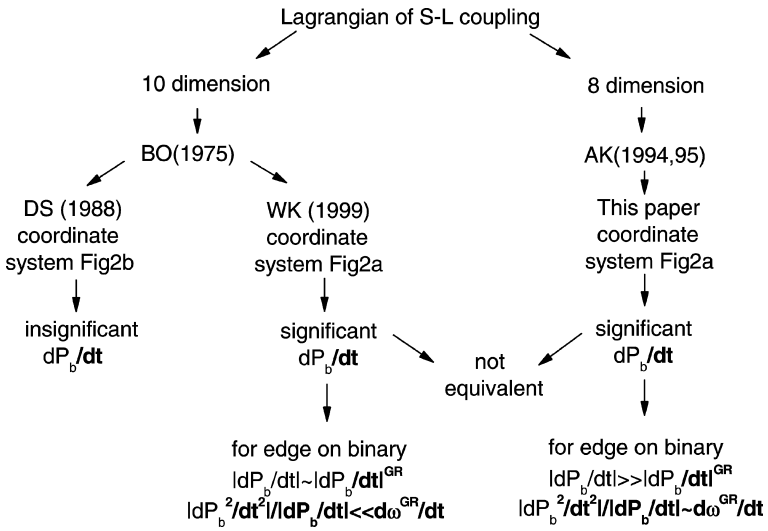


**Fig. 3** Relationship of the three expressions of the S-L coupling induced orbital effects.

## 7 CONFRONTATION WITH OBSERVATION

The precise timing measurement on two typical binary pulsars, PSR J2051–0827 and PSR J1713+0747, provides evidence on whether $\dot{\omega}^S$ and $\dot{P}_b$ is 1PN or 1.5PN, but it still difficult to distinguish which 1PN effect is valid, WK or this paper.

The orbital motion causes a delay of $T = \boldsymbol{r}_1 \cdot \boldsymbol{K}_0/c = r_1(t) \sin \omega^{\rm obs}(t) \sin i(t)/c$ in the pulse arrival time, where $\boldsymbol{r}$ is the pulsar position vector and $\boldsymbol{K}_0$ is the unit vector of the line of sight. The residual $\delta T = \boldsymbol{r}_1 \cdot \boldsymbol{K}_0/c - (\boldsymbol{r}_1 \cdot \boldsymbol{K}_0/c)_K$ of the time delay compared with the Keplerian value is of interest (Lai et al. 1995). Averaging over one orbit $r \approx a$, and in the case $t \ll 1/|\dot{\omega}^{\rm obs}|$, the S-L coupling induced residual is,

$$\begin{aligned}\delta T &= \frac{a_p}{c} \cos i \frac{di}{dt} t \sin \omega^{\rm obs} + \frac{\dot{a}_p \sin i}{c} t \sin \omega^{\rm obs} + \frac{a_p \sin i}{c} \dot{\omega}^{\rm obs} t \cos \omega^{\rm obs} \\ &= \dot{x}_1 t \sin \omega^{\rm obs} + \frac{\dot{a}}{a} x t \sin \omega^{\rm obs} + \dot{\omega}^{\rm obs} x t \cos \omega^{\rm obs} \ . \end{aligned} \tag{78}$$

By Eq. (A1), we have $\dot{a}/a \sim J/a^3 \sim \dot{\omega}^{\rm obs}$. Therefore, the second and third term on the right side of Eq. (78) cannot be distinguished in the current treatment of pulsar timing. In other words, the effect of $\dot{a}$ can be absorbed in $\dot{\omega}^{\rm obs}$.

### 7.1 PSR J2051–0827

As discussed above, the second term at the right side of Eq. (59) can be absorbed by $\dot{\omega}^{\rm obs}$, therefore, $\dot{x} \approx \dot{x}_1$, and by Eq. (57) we have

$$\dot{\Omega} = -\frac{\dot{x}}{x} \frac{\tan i}{\sin \lambda_{LJ} \sin \Omega_0} = -\frac{di}{dt} \frac{1}{\sin \lambda_{LJ} \sin \Omega_0} \ . \tag{79}$$

According to optical observations, the system is likely to be moderately inclined with an inclination angle $i \sim 40^\circ$ (Stappers et al. 2001). By the measured results of $x = 0.045\,{\rm s}$,

$\dot{x} = -23(3) \times 10^{-14}$ (Doroshenko et al. 2001), and by assuming $\sin\lambda_{LJ}\sin\Omega_0 = 2 \times 10^{-3}$, Eq. (79) can be written in magnitude,

$$\dot{\Omega} = \Big(\frac{\dot{x}}{2.3\times10^{-13}}\Big)\Big(\frac{x}{0.045}\Big)^{-1}\Big(\frac{\tan i}{\tan 40^\circ}\Big)\Big(\frac{\sin\lambda_{LJ}\sin\Omega_0}{2\times10^{-3}}\Big)^{-1} \sim 2\times10^{-9}\,(\mathrm{s}^{-1}) \quad . \tag{80}$$

In the following estimations in this section all values are absolute values. By Eq. (51) we can assume $\ddot{\omega}^S \sim (\dot{\omega}^S)^2 \sim \dot{\Omega}^2 \approx 4\times10^{-18}$. Usually $\ddot{\omega}^S$ can vary over a large range, i.e., $\ddot{\omega}^S > (\dot{\omega}^S)^2$, depending on the combination of parameters, such as binary parameters, magnitude and orientation of $S_1$ and $S_2$. In this paper we assume that $\ddot{\omega}^S \sim (\dot{\omega}^S)^2$. Then from Eq. (69) we have

$$\dot{P}_b = \frac{1}{2\pi}\Big(\frac{\ddot{\omega}^S}{4\times10^{-18}}\Big)\Big(\frac{P_b}{0.099\,\mathrm{d}}\Big)^2 \sim 5\times10^{-11}(\mathrm{s\,s}^{-1}) \quad . \tag{81}$$

By Eq. (64) we can estimate $d^3\omega^S/dt^3 \sim \dot{\Omega}^3 \approx 8\times10^{-27}\,\mathrm{s}^{-3}$, and similarly we can estimate $d^4\omega^S/dt^4 \sim \dot{\Omega}^4 \approx 16\times10^{-36}\,\mathrm{s}^{-4}$. Hence, by Eqs. (70) and (71) we have $\ddot{P}_b \sim 9\times10^{-20}\,\mathrm{s}^{-1}$ and $d^3P_b/dt^3 \sim 2\times10^{-28}\,\mathrm{s}^{-2}$. By Eqs. (59) and (60), $\ddot{x}/\dot{x} \sim \dot{\Omega} \sim 2\times10^{-9}\mathrm{s}^{-1}$, which is consistent with the observations as shown in Table 2.

**Table 2** Measured parameters compared with the geodetic precession induced ones in PSR J2051−0827

| Observation | WK & this paper |
|---|---|
| $\dot{x}^{\mathrm{obs}} \approx -23(3)\times10^{-14}$ | $\dot{x} = \dot{x}^{\mathrm{obs}}$ |
| $(\ddot{x}/\dot{x})^{\mathrm{obs}} \le -3.0\times10^{-9}\mathrm{s}^{-1}$ | $\lvert\ddot{x}/\dot{x}\rvert \approx 2\times10^{-9}\mathrm{s}^{-1}$ |
| $\dot{P}_b^{\mathrm{obs}} = -15.5(8)\times10^{-12}$ | $\lvert\dot{P}_b\rvert = \lvert\frac{\ddot{\omega}^S P_b^2}{2\pi}\rvert \sim 5\times10^{-11}$ |
| $\ddot{P}_b^{\mathrm{obs}} = 2.1(3)\times10^{-20}\mathrm{s}^{-1}$ | $\lvert\ddot{P}_b\rvert = \lvert\frac{P_b^2}{2\pi}\frac{d^3\omega^S}{dt^3}\rvert \sim 9\times10^{-20}\mathrm{s}^{-1}$ |
| $\frac{d^3P_b^{\mathrm{obs}}}{dt^3} = 3.6(6)\times10^{-28}\mathrm{s}^{-2}$ | $\lvert\frac{d^3P_b}{dt^3}\rvert = \lvert\frac{P_b^2}{2\pi}\frac{d^4\omega^S}{dt^4}\rvert \sim 2\times10^{-28}\mathrm{s}^{-2}$ |

Therefore, once $\dot{x}$ is in agreement with the observation, the corresponding $\dot{\omega}^S$ can make the derivatives of $P_b$ consistent with the observation as shown in Table 2. In contrast, the effect derived from Damour & Schäfer's equation cannot explain the significant derivatives of $P_b$.

### 7.2 PSR J1713+0747

By the measured parameters, $x = 32.3\,\mathrm{s}$, $|\dot{x}| = 5(12)\times10^{-15}$, $i = 70^\circ$ (Camilo et al. 1994), and by assuming $\sin\lambda_{LJ}\sin\Omega_0 = 1\times10^{-4}$, we have, in order of magnitude,

$$\dot{\Omega} = \Big(\frac{\dot{x}}{5\times10^{-15}}\Big)\Big(\frac{x}{32.3}\Big)^{-1}\Big(\frac{\tan i}{\tan 70^\circ}\Big)\Big(\frac{\sin\lambda_{LJ}\sin\Omega_0}{1\times10^{-4}}\Big)^{-1} \sim 4\times10^{-12}(\mathrm{s}^{-1}) \quad , \tag{82}$$

and similarly we have

$$\dot{P}_b = \frac{1}{2\pi}\Big(\frac{\ddot{\omega}^S}{16\times10^{-26}}\Big)\Big(\frac{P_b}{67.8\,\mathrm{d}}\Big)^2 \sim 1\times10^{-10}(\mathrm{s\,s}^{-1}) \quad . \tag{83}$$

A comparison of the observed and predicted variabilities is shown in Table 3. The variabilities are shown to be well consistent with one another. Note that $\dot{x}^{\mathrm{obs}}$ and $\dot{P}_b^{\mathrm{obs}}$ measured in these two typical binary pulsars cannot be interpreted by the gravitational radiation induced $\dot{x}$ and $\dot{P}_b$, since they are 3 or 4 order of magnitude apart.

**Table 3** Measured values in PSR J1713+0747 compared with the calculated, geodetic precession induced values

| Observation | WK & this paper |
|---|---|
| $\lvert\dot{x}\rvert^{\rm obs} = 5(12)\times 10^{-15}$ | $\dot{x} = \dot{x}^{\rm obs}$ |
| $\dot{P}_b^{\rm obs} = 1(29)\times 10^{-11}$ | $\lvert\dot{P}_b\rvert = \lvert\frac{\ddot{\omega}^S P_b^2}{2\pi}\rvert \sim 1\times 10^{-10}$ |

### 7.3 PSRs J0737–3039 A and B

PSRs J0737–3039 A and B is a double-pulsar system with $P_b = 0.102251563(1)$day, advance of periastron, $\dot{\omega} = 16.90(1)\,\deg\ {\rm yr}^{-1}$ and orbital inclination angle $i = 87.7^{+17}_{-29}$ (Burgay et al. 2003; Lyne et al. 2004). This binary pulsar system with $i \approx \pi/2$ may tell us not only whether $\dot{\omega}^S$ and $\dot{P}_b$ are significant or not, but also which one of the two (WK or this paper) is valid.

As given by Eq. (63) the measured $\dot{\omega}$ is the sum of the relativistic advance of periastron and the S-L coupling induced advance of periastron,

$$\dot{\omega}^{\rm obs} = \dot{\omega}^{\rm GR} + \dot{\omega}^S = 16.90 \quad (\deg\ {\rm yr}^{-1}) \ . \tag{84}$$

where $\dot{\omega}^{\rm GR}$ and $\dot{\omega}^S$ are both 1PN. In order of magnitude one can estimate

$$\dot{\omega}^S \sim \dot{\omega}^{\rm obs} = 16.90 \quad (\deg\ {\rm yr}^{-1}) \ . \tag{85}$$

Thus we have $\ddot{\omega}^S \sim (\dot{\omega}^S)^2 \approx 8.8\times 10^{-17}{\rm s}^{-2}$. If the eccentricity of PSRs J0737–3039 A and B is neglected, then in the same way as PSR J2051–0827 and PSR J1713+0747, we have

$$\dot{P}_b = \frac{1}{2\pi}\Big(\frac{\ddot{\omega}^S}{8.8\times 10^{-17}}\Big)\Big(\frac{P_b}{0.1\,{\rm d}}\Big)^2 \sim 1\times 10^{-9}({\rm s\,s}^{-1}) \ . \tag{86}$$

The treatment $\dot{\omega}^S \sim \dot{\omega}^{\rm obs}$ and $\ddot{\omega}^S \sim (\dot{\omega}^S)^2$ might over estimate the S-L coupling induced $\dot{P}_b$ by one or even two orders of magnitude. Nevertheless, the S-L coupling induced $\dot{P}_b$ is likely to be much larger than that caused by the gravitational radiation, $\dot{P}_b^{\rm GR} = -1.2\times 10^{-12}\ {\rm s\,s}^{-1}$ (Burgay et al. 2003). Since the observational $\dot{P}_b$ will be given soon, whether $\dot{P}_b$ is significant or not can be tested on this binary pulsar system.

The particular orbital inclination of this binary pulsar system can tell us more about the S-L coupling induced effects. With $i = 87.7^{+17}_{-29}$ for this system, we have $\cot i \approx 0.04$, WK's $\dot{\omega}^S$ given by Eq. (73) should be much smaller than this paper's $\dot{\omega}^S$ given by Eq. (72). Thus we have two ways of testing the validity of the S-L coupling effect given by WK and by this paper.

The first is by means of $\ddot{\omega}^S \sim (\dot{\omega}^S)^2 \propto (\cot i)^2$, and $\dot{P}_b \propto (\dot{\omega}^S)^2$. We find $(\dot{P}_b)_{\rm WK} \sim (\cot i)^2\dot{P}_b$. Thus the magnitude of $\dot{P}_b$ corresponding to WK's value should not exceed $1.6\times 10^{-12}$ ${\rm s\,s}^{-1}$, which is close to the gravitational wave induced $\dot{P}_b$.

In other words if the measured magnitude of $\dot{P}_b$ of PSRs J0737–3039 A and B is not much larger than the gravitational wave induced $\dot{P}_b$, then the expression of this paper can be excluded.

The second is based on Eqs. (69)–(71), from which we have

$$\frac{|\dddot{P}_b|}{|d^3P_b/dt^3|} \sim \frac{|\dot{P}_b|}{|\ddot{P}_b|} \sim \frac{1}{|\dot{\omega}^S|} \, . \tag{87}$$

For WK, $\dot{\omega}^S$ is nearly two orders of magnitude smaller than the relativistic advance of periastron, $\dot{\omega}^{\rm GR}$; for this paper, they are of the same order of magnitude. Therefore, if the ratio of Eq. (87) is close to $1/\dot{\omega}^{\rm GR}$ then this paper is supported. Precise measurement of the derivative

of $P_b$ in this binary pulsar system may show which is favored. Actually Eq. (86) is one way of absorbing the Spin-Orbit coupling induced $\ddot{\omega}^S$. This effect can be attributed to the spin period, $P$, to $\ddot{\omega}^S$ itself, or to other parameters. However, the relation of Eq. (87) still hold in such cases, the difference is that the derivative and derivatives of $P_b$ are replaced by that of other parameters.

## 8 DISCUSSION AND CONCLUSIONS

BO and AK's orbital precession velocity has been treated as equivalent, since BO and AK gave equivalent torque, $\dot{\boldsymbol{L}}$, as shown in Eqs. (9) and (18) respectively. However, Eqs. (9) and (18) actually correspond to two different orbital precession velocities, Eqs. (12) and (19), this is because the same torque can cause different effects when the dynamic system is calculated under different dimensions. BO's orbital precession velocity was obtained for a system of 10; while AK's, for eight dimensions. The former violates the triangle constraint and the latter satisfies it.

The difference in physics leads to difference in observable effects. Eqs. (12) and (19) correspond to different combinations of $\Omega$ and $\omega$ ($\Omega$ and $\omega$ are defined in Fig. 2), and since the observational effect depends on $\Omega$ and $\omega$, rather than on $\dot{\boldsymbol{L}}$, the equivalent value in $\dot{\boldsymbol{L}}$ may correspond to different observational effects. Specifically, BO and AK gave the same $\Omega$, but different $\omega$ (note that $\Omega$ and $\omega$ are components of the vectors given by Eqs. (12) or (19)). By Eqs. (61) and (62), the observed advance of periastron depends on both $\Omega$ and $\omega$, thus BO and AK must correspond to different observational effects.

In the calculations of Sections 4 and 5, we can see the influence of the dimension and physical constraint on the results of the equation of motion, perturbation and observational effects.

The S-L coupling induced precession of orbit can cause an additional time delay to the time of arrival (TOA), which can be absorbed in the orbital period. Since the additional time delay itself is a function of time, a change in the orbital period, $\dot{P}_b$, appears. Actually $\dot{P}_b$ corresponds to $\ddot{\omega}^S$ as shown in Eq. (69), which cannot be absorbed by $\dot{\omega}^{\rm GR}$ ($\dot{\omega}^S$ can be absorbed by $\dot{\omega}^{\rm GR}$). Therefore, the higher order derivatives of orbital period provide a good means of testing different models. The observation of $\dot{P}_b$, $\ddot{P}_b$ and $d^3P_b/dt^3$ in PSR J 2051–0827 supports significant S-L coupling induced effects.

This paper for the first time points out that WK's expression actually corresponds to significant $\dot{\omega}^S$ and $\dot{P}_b$ which, however are not equivalent to the significant $\dot{\omega}^S$ and $\dot{P}_b$ given by this paper. Precise measurement of $\dot{P}_b$, $\ddot{P}_b$ and $d^3P_b/dt^3$ of specific binary pulsars with orbital inclination $i \to \pi/2$, like PSRs 0737–3039 A and B, may provide a test of the discrimination between WK and this paper.

**Acknowledgements** I thank T. Huang for help in clarifying the theoretical part of this paper. I thank R.N. Manchester for his help in understanding pulsar timing and measurement. I thank T. Lu for useful comments during this work. I thank W.T. Ni and C.M. Xu for useful suggestions in the presentation of this paper. I thank E.K. Hu, A. Rüdiger, K.S. Cheng, N.S. Zhong, and Z.G. Dai for continual encouragement and help. I also thank Y. Li, Z.X. Yu, C.M. Zhang, L. Zhang, Z. Li, H. Zhang, S.Y. Liu, X.N. Lou, X.S. Wan for useful discussions.

## APPENDIX

By $\widetilde{S} = \boldsymbol{a}_{so} \cdot \hat{\boldsymbol{n}}$ and $T = \boldsymbol{a}_{so} \cdot \hat{\boldsymbol{t}}$, $\frac{d\Omega}{dt}$ and $\frac{d\omega}{dt}$ have been given by Eqs. (45), (46), (49) and (51), following the standard procedure for computing perturbations of orbital elements Roy (1991). Similarly, four other elements can be given:

$$\frac{da}{dt} = \frac{2}{n\sqrt{1-e^2}}(\widetilde{S}e\sin f + \frac{p\widetilde{T}}{r}) \ , \tag{A1}$$

$$\left\langle \frac{da}{dt} \right\rangle = \frac{\sigma_1 J(1+e^2)}{(1-e^2)^{5/2}a^2}(P_y Q_x - P_x Q_y) \ , \tag{A2}$$

$$\frac{de}{dt} = \frac{\sqrt{1-e^2}}{na}[\widetilde{S}\sin f + \widetilde{T}(\cos E + \cos f)] \ , \tag{A3}$$

$$\left\langle \frac{de}{dt} \right\rangle = \frac{\sigma_1 Je}{(1-e^2)^{3/2}a^3}(P_y Q_x - P_x Q_y) \ , \tag{A4}$$

$$\frac{d\lambda_{LJ}}{dt} = \frac{\widetilde{W}r\cos(\omega+f)}{na^2\sqrt{1-e^2}}\frac{1}{\sin\lambda_{LJ}} \ , \tag{A5}$$

$$\begin{aligned}\left\langle \frac{d\lambda_{LJ}}{dt} \right\rangle = {} & \frac{3\cos\lambda_{LJ}}{2a^3(1-e^2)^{3/2}\sin\lambda_{LJ}}(P_z\cos\omega + Q_x\sin\omega)[(P_yQ_z - P_zQ_y)(S_x\sigma_1 + S_{2x}\sigma_2) \\ & +(P_zQ_x - P_xQ_z)(S_y\sigma_1 + S_{2y}\sigma_2) + (P_xQ_y - P_yQ_x)(S_z\sigma_1 + S_{2z}\sigma_2)] \ ,\end{aligned} \tag{A6}$$

$$\frac{d\epsilon}{dt} = \frac{e^2}{1+\sqrt{1-e^2}}\frac{d\varpi}{dt} + 2\frac{d\Omega}{dt}(1-e^2)^{1/2}(\sin^2\frac{\lambda_{LJ}}{2}) - \frac{2r\widetilde{S}}{na^2} \ , \tag{A7}$$

where

$$\frac{d\varpi}{dt} = \frac{d\omega'}{dt} + 2\frac{d\Omega}{dt}\Big(\sin^2\frac{\lambda_{LJ}}{2}\Big) \ ,$$

$$\left\langle \frac{d\epsilon}{dt} \right\rangle = \frac{e^2}{1+\sqrt{1-e^2}}\left\langle \frac{d\varpi}{dt} \right\rangle + 2\left\langle \frac{d\Omega}{dt} \right\rangle(1-e^2)^{1/2}\Big(\sin^2\frac{\lambda_{LJ}}{2}\Big) - \frac{\sigma_1 J}{a^3(1-e^2)}(P_yQ_x - P_xQ_y) \ . \tag{A8}$$

### References


Apostolatos T. A., Cutler C., Sussman J. J., Thorne K. S., 1994, Phys. Rev. D, 49, 6274
Barker B. M., O'Connell R. F., 1975, Phys. Rev. D, 12, 329
Burgay M. et al., 2003, Nature, 426, 531
Camilo F., Foster R. S., Wolszczan A., 1994, ApJ, 437, L39
Damour T., Schäfer G., 1988, IL Nuovo Cimento, 101B, 127
Doroshenko O., Löhmer O., Kramer M., Jessner A., Wielebinski R., Lyne A. G., Lange Ch., 2001, A&A, 379, 579
Hamilton A. J. S., Sarazin C. L., 1982, MNRAS, 198, 59
Kidder L. E., 1995, Phys. Rev. D, 52, 821
Kopeikin S. M., 1996, ApJ, 467, L93
Lai D., Bildsten L., Kaspi V., 1995, ApJ, 452, 819
Liu L., 1993, Method in Celestial Mechanics, Nanjing University Press
Lyne A. G. et al., 2004, Science, 303, 1153
Roy A. E., 1991, Orbital motion, Adam Hilger
Smarr L. L., Blandford R. D., 1976, ApJ, 207, 574
Stappers B. W., Van Kerkwijk M. H., Bell J. F., Kulkarni S. R., 2001, ApJ, 548, L183
Wex N., Kopeikin S. M., 1999, ApJ, 514, 388
Yi Z. H., 1993, Essential Celestial Mechanics, Nanjing University Press